Volume 336, number 1, 148–152 FEBS 13394 December 1993

Crystallization and crystallographic investigations of ribonucleotide reductase protein R1 from *Escherichia coli*

Ulla Uhlin, Tomas Uhlin, Hans Eklund*

Department of Molecular Biology, Swedish University of Agricultural Sciences, Uppsala Biomedical Center, Box 590, S-751 49 Uppsala, Sweden

Received 15 October 1993; revised version received 3 November 1993

Crystals of *Escherichia coli* ribonucleotide reductase protein R1 have been grown in complex with a synthetic peptide corresponding to the carboxyl end of protein R2. Good quality crystals could only be obtained after improvement of the purification protocol and are of the space group R32 with hexagonal cell axes $a = b = 226$ Å and $c = 341$ Å. They contain 3 subunits per asymmetric unit and diffract to 2.5 Å resolution in synchrotron radiation. A multiple isomorphous replacement map at 5.5 Å, improved by solvent flattening, shows that the dimeric molecules are elongated, about 110 Å long. The dimer is thin in the middle around the molecular two-fold axis. The subunit is shaped like a bowl, probably with the active site in its center.

Crystallization; Ribonucleotide reductase; Protein purification; Peptide complex; Crystal packing; Heavy atom derivative

1. INTRODUCTION

Ribonucleotide reductase (RNR) is an essential enzyme for DNA synthesis. It catalyses the reduction of all four ribonucleotides to their corresponding deoxyribonucleotides [1]. In *Escherichia coli* and higher organisms RNR consists of two homodimeric unequal proteins R1 and R2 (for reviews see [2–4]). A catalytically active enzyme is formed by a one to one complex of the two proteins in the presence of Mg^{2+} and ATP. The carboxyl end of R2 contributes to a large extent to the binding between the two proteins, and peptides of the carboxyl end of R2 have been shown to inhibit formation of the active holoenzyme [5–8].

Each subunit of the protein R1 has two different effector binding sites for allosteric regulation. One site regulates the overall activity with ATP and dATP as effectors while the other site regulates substrate specificity with deoxyribonucleoside triphosphates as effectors. R1 also contains redox active cysteines which become oxidized during catalytis. To regenerate active enzyme, this disulfide bridge has to be reduced. This can be done by at least two different systems, the glutaredoxin and thioredoxin systems [9].

The R1 protein is about twice as large as the R2 protein in most species. In *E. coli*, R1 has a molecular weight of 2×83 kDa where each peptide consists of 761 amino acid residues [10]. The smaller R2 protein (2×43.4 kDa) contains a tyrosyl free radical close to a binuclear iron center [11].

*Corresponding author.

For several years we have worked on the structure determination of ribonucleotide reductase from *E. coli*. The main difficulty of this work has been to obtain useful crystals for crystallographic studies. The R1 protein has been crystallized in at least ten different crystal forms, and R2 in three orthorhombic crystal forms [12]. Most of the crystal forms were not suitable for high-resolution crystallography. Crystals of the holoenzyme have been obtained, but they have large cell dimensions and are X-ray sensitive and thus not useful for structure determination. By extensive exploration of different crystallization conditions in combination with improved enzyme preparation we were able to obtain crystals of good quality of the R2 protein [12]. With this crystal form the three-dimensional structure of R2 could be solved at 2.2 Å resolution [13].

Most of the different crystal forms of R1 contain a large number of subunits per asymmetric unit, and are generally sensitive to X-ray radiation. Some of the crystal forms could only be obtained from one single enzyme preparation. This paper will describe a new, improved purification method for R1, crystallization of a complex of R1 and a 20-residues-long peptide corresponding to the carboxyl end of R2, and crystallographic investigations of the resulting rhombohedral crystal form.

2. MATERIALS AND METHODS

Protein R1 was purified from the overproducing strain C600/pLHS1 [14]. In the new enzyme purification procedure, the protocol was followed as described in [15,16] to the step after the ammonium sulphate precipitation. The crude precipitate was dissolved in 50 mM Tris buffer pH 7.6 and frozen with 10% glycerol in 1 ml portions. A

 Published by Elsevier Science Publishers B.V.

column was packed with Phenyl-Sepharose CL4B (Pharmacia) (1.6 × 11 cm), and connected to an FPLC-system. After equilibration with 0.75 M ammonium sulphate, 1 ml of the sample was thawed and mixed with 1 ml 1.5 M ammonium sulphate before injection. The separation protocol involved two consecutive 120-min linear gradients. The first gradient was run from 0.75 M ammonium-sulphate to 50 mM Tris pH 7.6 and 5 mM DTT, and the other from 50 mM Tris-buffer pH 7.6 with 5 mM DTT to distilled water containing 3 mM DTT. The flow rate was set to 1 ml/min and 1-ml fractions were collected. Tris buffer pH 7.6 (15 μl of 1 M) was immediately added to each 1 ml fraction (Fig. 1). Centricon (Amicon) was used to concentrate and change buffer on the purified protein, before addition of the peptide for crystallization.

The 20-residue peptide (Y L V G Q I D S E V D T D D L S N F Q L) corresponding to the carboxyl end of R2 was synthesized by the solid-phase peptide synthesis procedure using an applied Biosystems 430A Synthesizer. Freeze-dried peptide (20 mg) was dissolved in 200 μl 10 mM Tris solution with pH approximately 10. The pH was lowered to 6.5 with 100 μl 25 mM sodium citrate pH 6.0. For desalting a 2 ml G25 column equilibrated with 25 mM sodium citrate buffer pH 6.0 was used.

The best crystals are obtained using the hanging drop method with droplets of 10 μl (5 μl protein mixture and 5 μl well solution). Culture cells (Costar) are used with a one ml well solution of 17% lithium sulphate and 10 mM magnesium sulphate in buffer (25 mM sodium citrate pH 6.0). (All chemicals were from Merck). A concentrated protein solution is adjusted to a concentration of 30 mg/ml in buffer and diluted to 15 mg/ml with the peptide solution. For good crystal growth, a 20-fold molar excess of the peptide is needed. The protein mixture is incubated at +5°C for half an hour before crystallization, and crystals grow at the same temperature within one week (Fig. 2).

Space group determination was performed using precession and oscillation films and the Buddha auto-indexing program written by M. Blum [17]. Data have been processed in space group R32 with hexagonal cell axes $a = b = 226$ Å and $c = 341$ Å. The corresponding rhombohedral cell has the cell dimensions $a = b = c = 173$ Å and $\alpha = \beta = \gamma = 82°$. The crystals diffract to about 2.5 Å in synchrotron radiation.

Native and heavy atom derivative data were collected on a Xentronics multiwire area detector (Nicolet) on a Rigaku rotating anode source. Native data at higher resolution have also been collected at the synchrotron (station X31, EMBL) in Hamburg (Table I). Data reduction and scaling were performed with the CCP4 program suite (Daresbury, England).

Patterson maps were investigated using a real space Patterson search program (RSPS) written by S. Knight [18]. The derivative with the metal cluster Ta_6Br_{14} gave a difference Patterson map that was possible to solve with three sites per asymmetric unit. Phases from this derivative were good enough to allow us to find heavy atom positions in other derivatives that were consistent with their difference Patterson maps.

Heavy atom parameters, from four derivatives, were further refined in Heavy [19], first against the origin removed Patterson maps and then using lack of closure refinement. Some statistics from the refinement to 5.5 Å are shown in Table I.

To test binding of heavy atom labeled peptide, the tyrosine was iodinated and the iodinated peptide was purified on a prepacked FPLC column, Pep-RPC, from Pharmacia. No crystals were obtained from crystallizations using mono- and diiodinated peptides. A longer peptide (22 residues) with a Cys and Ser added at the N-terminus was labeled with mercury and used in the same crystallization procedure but no crystals were obtained.

Calculation of the solvent content [20] indicated three or four monomers in one asymmetric unit. Three subunits would give a V_m of 3.4, while four subunits would give a V_m of 2.4. From the MIR map at 5.5 Å resolution it was clear that the asymmetric unit contained three subunits; the protein and solvent regions were obvious (Fig. 3a). The V_m for three subunits per asymmetric unit corresponds to a relatively high solvent content of 63%. The phases were further improved by solvent flattening [21] (Fig. 3b). From this map a skeletonized representation of the molecule was calculated using the bones option in O [22,23]. The bone atoms were assigned to different subunits and coloured. A bones representation of one R1 dimer is shown in Fig. 4. The crystal packing of the R1-dimers, and the choice of the three subunits in the asymmetric unit is shown in Fig. 5a,b. From the relations between the three subunits in the asymmetric unit, phases can be further improved by three-fold averaging [24].

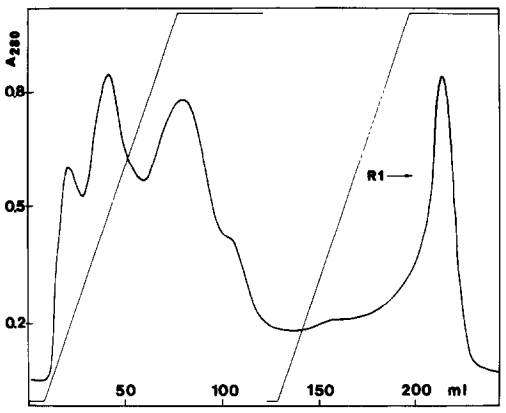

Fig. 1. Elution profile from the phenyl-sepharose column. In the first elution gradient ammonium sulphate is substituted by Tris-buffer, in the second gradient the Tris-buffer is substituted by distilled water.

3. RESULTS AND DISCUSSION

Two of the earlier obtained crystal forms of the R1 protein have been suitable for further crystallographic studies: one hexagonal form (P622) with cell dimensions $a = b = 96$ Å and $c = 220$ Å, and a monoclinic form (C2) with cell parameters $a = 211.5$ Å, $b = 119.6$ Å, $c = 129.5$ Å and $\beta = 123.9°$. Both crystal forms were grown with lithium sulphate as precipitant and contain one and two subunits per asymmetric unit, respectively. Unfortunately, these crystals could only be obtained from single R1 preparations and we have only managed to collect native data to 3.0 Å for these crystal forms so far.

Our R32 crystal form was obtained by using an improved fast enzyme preparation and by adding a synthetic polypeptide to the protein solution. The peptide

Fig. 2. Crystals of the ribonucleotide reductase R1 protein complex with a 20-residue-long peptide from the carboxyl end of R2. The largest crystal has a size of 0.7 × 0.6 × 0.4 mm.

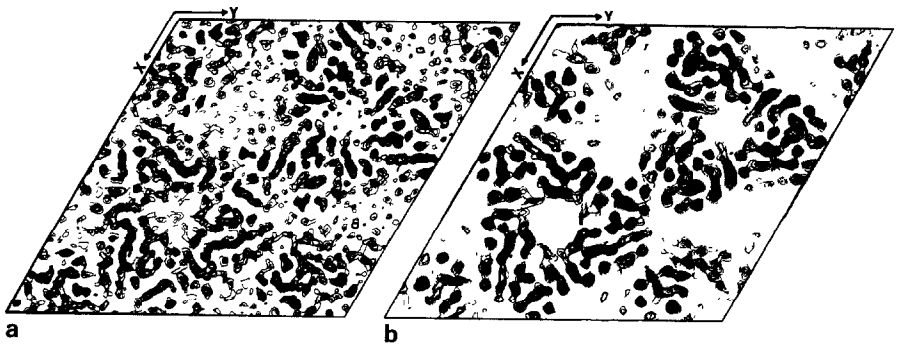

Fig. 3. Comparison of an 8 Å layer in the *c*-direction at 5.5 Å resolution (1 σ cut) of (a) the MIR map and (b) the solvent flattened map.

added has a length of 20 residues and the same sequence as the C-terminal residues of the R2 protein. The remaining crystallization conditions are similar to those used for growing the hexagonal (P622) and monoclinic (C2) crystals mentioned above.

The main difference between the new and the old enzyme preparation protocol is that one desalting and two ion-exchange separation steps are replaced by a purification step on a Phenyl-Sepharose column. In the final protocol the purification time is reduced to 1/4 compared to the original protocol [15,16]. The new purification method gives active protein as pure as with the old method.

Crystals are only obtained from a narrow range of the purification: only the top fraction gives useful crystals. We also found that the age of the protein was an important parameter for crystallization and the use of fresh sample was necessary for obtaining crystals of good quality. If the purified protein has been stored in the freezer (−70°C) for more than three months no crystals can be obtained.

The many difficulties in the crystallization of the R1 protein may be related to the cysteines involved in the activity of the protein, to flexible parts in the protein, and to conformational changes. The R1 protein contains 11 cysteines per subunit that have to be kept reduced during purification. Mutation studies show that five of the cysteines are important for the activity of the enzyme [25–30]. Two of these are located close to the C-terminus of the protein and interact with thioredoxin or glutaredoxin. They have been suggested to be involved in transfer of reducing power from the surface to the active site.

We have tried to stabilize the protein by adding effec-

Table I

Datacollection and heavy atom refinement[1]

Data-set[2]	Resol (Å)	Reflections (no.)	Compl. (%)	R-sym (%)	Δ-iso[3] (%)	Soak[4] (mM/h)	Sites (no.)	Phasing[5] power F_H/ε	Centric[6] *R*-factor R_C
Native									
Nat1	3.0	46,000	70	4	–	–	–	–	–
Nat2	3.0	42,000	62	5	–	–	–	–	–
Nat3	2.7	82,000	90	9	–	–	–	–	–
Merged Nat1-3	2.7	84,000	92	10	–	–	–	–	–
Derivatives									
$KAu(CN)_2$	5.5	9,600	82	7	11	0.1/24	3	1.2	0.7
$K_2Pt(CN)_4$	5.5	9,200	78	3	17	10/26	3	1.7	0.8
Ta_6Br_{14}	5.5	6,600	56	7	21	0.5/20	3	2.3	0.9
Ta_6Br_{14}	5.5	5,500	47	5	20	0.5/20	3	2.0	0.7
UO_2Ac_2	5.5	6,800	58	5	19	5/95	8	1.8	0.9
UO_2Ac_2	5.5	7,100	61	4	13	5/44	8	1.6	0.8

[1] Statistics from Heavy. Total figure of merit; 0.78 (10,646 reflections).
[2] Data-sets Nat1, Nat2 and derivatives were collected on a Xentronics (Nicolet) area detector. Data Nat3 was collected on the image plate at the synchrotron station X31 in Hamburg.
[3] The derivatives were scaled against Nat1 using RSTATS.
[4] The crystals were soaked in the mother liquor, where the desired heavy metal solution was added to the appropriate concentration.
[5] F_H/ε (phasing power) = *r.m.s.*(F_H/*r.m.s.* (lack of closure, where F_H is the calculated heavy atom structure factor.
[6] $R_C = \{ \Sigma \| F_{H(obs)}| - |F_{H(calc)}\| / \Sigma |F_{H(obs)}| \}$

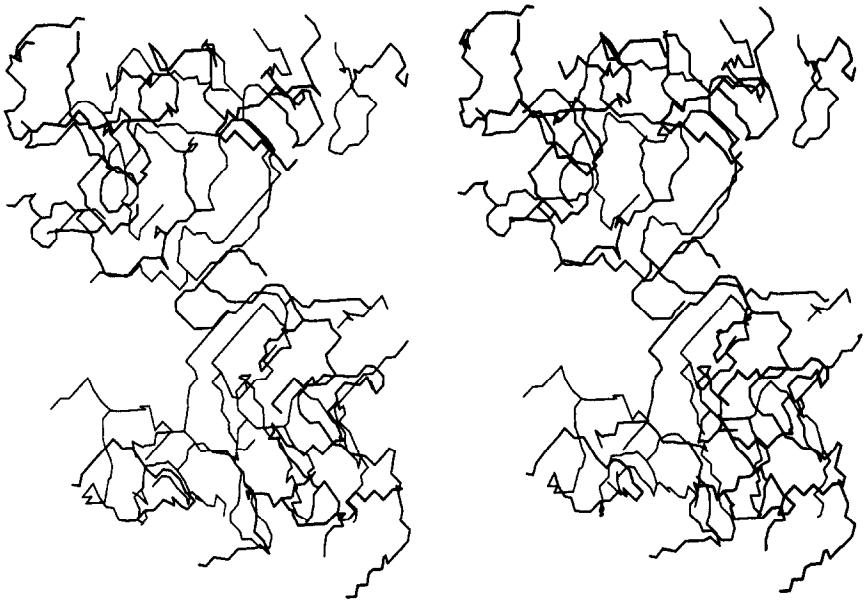

Fig. 4. Skeletonized representation of the R1 dimer viewed along the molecular two-fold axis. The closest three-fold axis is in the vertical direction in front of the dimer.

tors and inhibitors, but for various reasons most of the crystals obtained have not been suitable for crystallographic investigations. Most of the crystal forms have a large number of molecules in the asymmetric unit and/or are X-ray sensitive. Crystals of the R1 protein with the R2 20-mer are considerably more stable than any of the earlier obtained crystal forms. One crystal usually lasts for three days in the rotating anode beam and properly aligned it gives one full data-set to 3 Å.

Inhibition of activity with C-terminal peptides from R2 has been investigated, and the 20-residues-long peptide used in our investigation is known to strongly inhibit the specific activity of *E. coli* RNR [8]. The dissociation constant is 0.09 mM. The amount of peptide in our crystallizations is thus sufficient for formation of a complex of R1 and the added 20-residue peptide.

Seven different peptides, with lengths varying from 9 to 30 amino acids, were prepared and used under the same crystallization conditions as the 20-mer, but did not give any crystals. Our conclusion is, that the peptide in some way makes interactions important for the crystal packing and any shorter or longer peptides will cause unfavorable packing contacts.

The skeletonized representation of the R1 subunit has

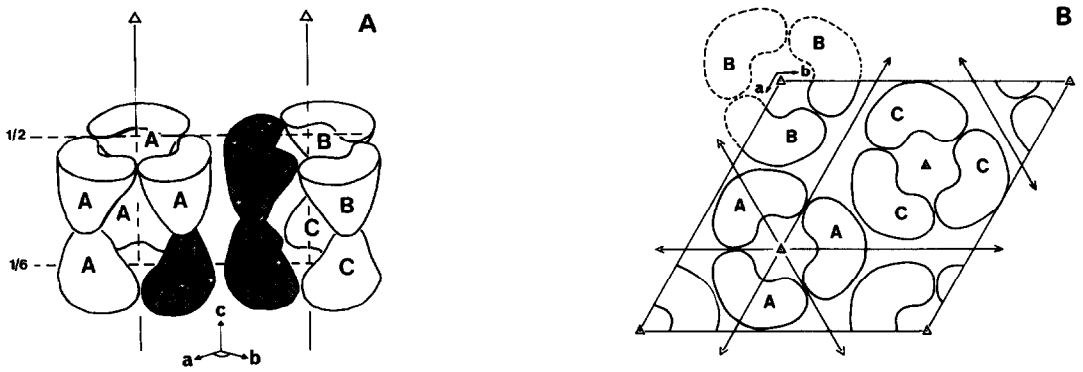

Fig. 5. Three R1 dimers cluster around the three-fold axes forming hexamers which stack on top of each other in three layers along the *c*-axis of the cell. The two unique hexamers are related by an approximate 3 Å translation and 20° rotation. For computational reasons, the three R1 subunits in the asymmetric unit are chosen close in space. One subunit is selected from one hexamer and one dimer from a nearby hexamer. Each hexamer has crystallographic three-fold symmetry, but the molecular dimer is related by a crystallographic two-fold axis in only one of the two hexamers. (a) Two hexamers are shown positioned around two threefold axes ($a = 2/3$, $b = 1/3$ and $a = 1/3$, $b = 2/3$) 1/6 to 1/2 along the *c*-axis. The non-crystallographically related subunits are marked A, B and C. Subunits chosen as the asymmetric unit are shaded. The top of the A subunits always pack against the bottom of the B subunits or vice versa, and subunit C against C. Subunits B–A have closer contact than C–C subunits. (b) The packing in the hexagonal plane. The two-fold axes shown are positioned in a plane on 1/3 of the *c*-axis, and the subunits illustrated here are located under this plane on 1/6–1/3 of the *c*-axis.

the shape of a large bowl and the two bowls that form the dimer are roughly perpendicular to each other. We suggest that the active site is located in the center of these bowls, where the main mercury and $Au(CN)_2^-$ sites are located since the active site is known to contain cysteine residues. The distance between the gold sites of the presumed active sites of the dimer is 43 Å.

The length of the dimeric molecule is about 110 Å and with a largest diameter of 75 Å. We have compared our R1 structure with the object observed by image analysis of two-dimensional R1 crystals [31]. Our suggestion is that the 110 Å object they interpreted as an R1 subunit more likely corresponds to one R1 dimer.

The dimer interaction is rather restricted. There seem to be more interactions within the crystallographic trimers than within the molecular dimers. We believe that the R2 dimer will fit in the cavities of the bowls and stabilize the R1 dimer while forming the holo-complex. A three-dimensional structure of the large subunit with a R2 peptide will be of help in understanding the formation of the RNR holo-complex. This is particularly interesting in view of the reports that the C-terminus of the RNR small protein from some viruses inhibits the formation of the RNR holoenzyme complex [6,7]. These virus encoded ribonucleotide reductases may serve as targets for anti-viral therapy [32].

Acknowledgements: We are grateful to Prof. Britt-Mari Sjöberg for the generous gift of recombinant bacteria and to her and her group for enzyme preparations in the earlier stages of this work. Many thanks to Dr. Gunnar Lindeberg who synthesized the peptides and Prof. Robert Huber for the gift of Ta_6Br_{14}. We also thank Erling Wikman for help with computers and Christer Andersson for keeping the area detector running. A special thanks to Pär Nordlund and Kyriacos Petratos for great help with data collection and data processing and we also thank all the helpful people at the EMBL lab in Hamburg. We are grateful to Dr. Pete Dunten for linguistic corrections of the manuscript.

REFERENCES

[1] Thelander and Reichard, P. (1979) Annu. Rev. Biochem. 48, 133–158.
[2] Eriksson, S. and Sjöberg, B.-M. (1989) in Allosteric Enzymes (Hervé, G., Ed.) pp. 189–215, CRC Press, Cleveland.
[3] Stubbe, J. (1990) Adv. Enzymol. 63, 349–419.
[4] Fontecave, M., Nordlund, P., Eklund, H. and Reichard, P. (1992) Adv. Enzymol. 65, 147–183.
[5] Sjöberg, B.-M., Karlsson, M. and Jörnvall, H. (1987) J. Biol. Chem. 262, 9736–9743.
[6] McClements, W., Yamanaka, G., Garsky, V., Perry, H., Colonno, R. and Stein, R.B. (1988) Virology 162, 270–273.
[7] Paradis, H., Gaudreau, P., Brazeau, P. and Langelier, Y. (1988) J. Biol. Chem. 263, 16045–50.
[8] Climent, I., Sjöberg, B.-M. and Huang, C.Y. (1991) Biochemistry 30, 5164–5171.
[9] Holmgren, A. (1989) J. Biol. Chem. 264, 13463–13460.
[10] Nilsson, O., Åberg, A., Lundqvist, T. and Sjöberg, B.-M. (1988) Nucleic Acids Res. 16, 4174.
[11] Reichard, P. and Ehrenberg, A. (1983) Science 221, 514–519.
[12] Nordlund, P., Uhlin, U., Westergren, C., Joelson, T., Sjöberg, B.-M. and Eklund, H. (1989) FEBS Lett. 258, 251–254.
[13] Nordlund, P., Sjöberg, B.-M. and Eklund, H. (1990) Nature 345, 593–598.
[14] Larsson, Å. (1984) Acta Chem. Scand. B38, 905–907.
[15] Sjöberg, B.-M., Hahne, S., Karlsson, M., Jörnvall, H., Göransson, M. and Uhlin, B.E. (1986) J. Biol. Chem. 261, 5658–5662.
[16] Larsson, Å., Karlsson, M., Sahlin, M. and Sjöberg, B.-M. (1988) J. Biol. Chem. 263, 17780–17784.
[17] Blum, M., Metcalf, P., Harrison, S.C. and Wiley, D.C. (1987) J. Appl. Cryst. 20, 235–242.
[18] Knight, S. (1989) PhD Thesis Swedish Univeristy of Agricultural Sciences.
[19] Terwillinger, T.C. and Eisenberg, D. (1983) Acta. Crystallogr. A39, 813–817.
[20] Matthews, B.W. (1968) J. Mol. Biol. 33, 491–497.
[21] Wang, B.C. (1985) Methods Enzymol. 115, 90–112.
[22] Jones, T.A. and Thirup, S. (1986) EMBO J. 5, 819–822.
[23] Jones, T.A., Bergdoll, M. and Kjeldgaard, M. (1990) in: Crystallographic and Modeling Methods in Molecular Design (Bugg, C. and Ealick, S., Eds.) Springer New York, pp. 189–199.
[24] Bricogne, G. (1974) Acta Cryst. A30, 395–405.
[25] Åberg, A., Hahne, S., Karlsson, M., Larsson, Å, Ormö, M., Åhgren, A. and Sjöberg, B.-M. (1989) J. Biol. Chem. 264, 12249–12252.
[26] Lin, A., Ashley, G. and Stubbe, J. (1987) Biochemistry 26, 6905–6909.
[27] Mao, S.S., Jokuston, M.I., Bollinger, J.-M. and Stubbe, J. (1989) Proc. Natl. Acad. Sci. USA 86, 1485–1489.
[28] Mao, S.S., Holler, T.P., Yu, G.X., Bollinger, J.-M., Booker, S., Johnston, M.I. and Stubbe, J. (1992) Biochemistry 31, 9733–9743.
[29] Mao, S.S., Holler, T.P., Bollinger, J.-M., Yu, G.X., Johnston, M.I. and Stubbe, J. (1992) Biochemistry 31, 9744–9751.
[30] Mao, S.S., Yu, G.X., Chalfoun, D. and Stubbe, J. (1992) Biochemistry 31, 9752–9759.
[31] Ribi, H., Reichard, P. and Kornberg, R. (1987) Biochemistry 26, 7974–7979.
[32] Preston, V., Palfreyman, J. and Dutia, B. (1984) J. Gen. Virol. 66, 1581–1587.